Supplementary Material

Appendix 1

Here we show that independent inhibition by a single drug of two distinct steps (A and B) in the viral life cycle results in a non-linear median effect dose-response curve that infects upward. At high drug concentrations, the slope (*m*) of the overall dose-response curve approaches the sum of the slopes of the dose-response curves at steps A and B.

Suppose PIs inhibit two independent steps of life cycle, A and B. Let I_A be the IC_{50} for inhibition of step A and I_B by the IC_{50} for inhibition of step B.

From equation 1, we have for step A:

$$f_{uA} = \frac{1}{1+\left(D/I_A\right)^{m_A}} = \frac{I_A^{m_A}}{I_A^{m_A} + D^{m_A}}$$

For step B:

$$f_{uB} = \frac{1}{1+\left(D/I_B\right)^{m_B}} = \frac{I_B^{m_B}}{I_B^{m_B} + D^{m_B}}$$

By Bliss independence, $f_u = f_{uA} f_{uB}$

$$\frac{f_a}{f_u} = \frac{1-f_u}{f_u} = \frac{1-f_{uA}f_{uB}}{f_{uA}f_{uB}} = \frac{1}{f_{uA}f_{uB}} - 1 = \frac{(I_A^{m_A} + D^{m_A})(I_B^{m_B} + D^{m_B})}{I_A^{m_A} I_B^{m_B}} - 1$$

$$\log\left(\frac{f_a}{f_u}\right) = \log\left[\frac{(I_A^{m_A} + D^{m_A})(I_B^{m_B} + D^{m_B})}{I_A^{m_A} I_B^{m_B}} - 1\right]$$

$$\log\left(\frac{f_a}{f_u}\right) = \log\left[\frac{I_A^{m_A} I_B^{m_B} + D^{m_A} I_B^{m_B} + I_A^{m_A} D^{m_B} + D^{m_A} D^{m_B}}{I_A^{m_A} I_B^{m_B}} - 1\right]$$

$$\log\left(\frac{f_a}{f_u}\right) = \log\left[\frac{D^{m_A} I_B^{m_B} + I_A^{m_A} D^{m_B} + D^{m_A} D^{m_B}}{I_A^{m_A} I_B^{m_B}}\right]$$

$$\log\left(\frac{f_a}{f_u}\right) = \log\left(D^{m_A} I_B^{m_B} + I_A^{m_A} D^{m_B} + D^{m_A} D^{m_B}\right) - \log\left(I_A^{m_A} I_B^{m_B}\right)$$

At $D>>I_A,I_B$:

$$\log\left(\frac{f_a}{f_u}\right) \approx \log\left(D^{m_A} D^{m_B}\right) - \log\left(I_A^{m_A} I_B^{m_B}\right)$$

$$\log\left(\frac{f_a}{f_u}\right) \approx (m_A + m_B)\log(D) - \log\left(I_A^{m_A} I_B^{m_B}\right)$$

Thus at high D, the median effect plot of log (f_a/f_u) vs log D for the inhibition on infectivity will approach a slope of m_A+m_B.

Appendix 2

Formulae used in Table 1 and the calculation of error.

F_u and D are as defined previously (Equation 2) and $IC_{50}^{'}$ is the concentration of drug that achieved 50% inhibition of one round of replication in reference (2). To calculate the IC_{50}, the following formula was used:

$$\log\left[\left(1-f_u\right)/f_u\right]=m\log\left[\frac{D}{IC_{50}}\right] \qquad \text{Equation 2}$$

$$\log[(1-f_u)/f_u]=m\log\left[\frac{D}{IC_{50}^{'}}\times\frac{IC_{50}^{'}}{IC_{50}}\right]$$

$$=m\log\left[\frac{D}{IC_{50}^{'}}\right]+m\log\left[\frac{IC_{50}^{'}}{IC_{50}}\right]$$

Thus, plotting *log [(1-f_u)/f_u]* vs *log ($D/IC_{50}^{'}$)* will approximately linearize the dose-response curve. The y-intercept (*b*) is equivalent to $m\log\left[\frac{IC_{50}^{'}}{IC_{50}}\right]$. Therefore,

$$b=m\log\left[\frac{IC_{50}^{'}}{IC_{50}}\right]$$

$$IC_{50}=\frac{IC_{50}^{'}}{10^{b/m}} \qquad \text{Equation 5}$$

Microsoft Excel© LINEST function was used to calculate the line of best fit where unknown Y's and unknown X's were selected to be *log [(1-f_u)/f_u]* and *log ($D/IC_{50}^{'}$)*, respectively. In addition to the slope (m) and the y-intercept (*b*), this function returns the error in these values δm and δb.

The following formulae were used to calculate the other parameters in Table 1. The symbol δ indicates the error in each parameter.

$$\delta IC_{50}=\frac{IC_{50}\left(\frac{b}{m}\right)\sqrt{\left(\frac{\delta b}{b}\right)^2+\left(\frac{\delta m}{m}\right)^2}}{0.434} \qquad \text{Equation 6}$$

$$IIP_{C\max}=\log\left(1+\left(\frac{C_{\max}}{IC_{50}}\right)^m\right) \qquad \text{Equation 7}$$

$$\delta IIP_{C\max}=\delta m\log\left(\frac{C_{\max}}{IC_{50}}\right) \qquad (C_{max}>>IC_{50}) \qquad \text{Equation 8}$$

The fractional decrease in the inhibitory potential of the drug at C_{max} (ΔIIP_{cmax}) for each mutant clone compared to the wild type can be calculated as:

$$\Delta IIP_{c\max} = 1 - \frac{IIP_{clone,c\max}}{IIP_{wt,c\max}} \qquad \text{Equation 9}$$

where the inhibitory potential of the drug against the mutant clone at $Cmax$ is denoted as $IIP_{clone,cmax}$. The corresponding value for the wild type envelope is denoted as $IIP_{wt,cmax}$.

The error in ΔIIP_{cmax}, $\delta(\Delta IIP_{cmax})$ is calculated using Equation 10.

$$\delta(\Delta IIP_{c\max}) = \Delta IIP_{c\max} \sqrt{\left(\frac{\delta IIP_{clone,c\max}}{IIP_{clone,c\max}}\right)^2 + \left(\frac{\delta IIP_{wt,c\max}}{IIP_{wt,c\max}}\right)^2} \qquad \text{Equation 10}$$

The Replication Capacity of a clone (RC_{clone}) is calculated as follows:

$$RC_{clone} = \frac{f_{clone}}{f_{wt}} \qquad \text{Equation 11}$$

where f_{clone} and f_{wt} are defined as the fitness of the mutant clone and the wild type, respectively. Experimentally, they are measured as the percentage of GFP^+ cells observed when $CD4^+$ T cells are infected with each virus in the absence of any drug.

The Selective advantage of a given clone at a given dose (D) of the drug, is defined as follows:

$$SA = RC_{clone} \times 10^{(IIP_{wt} - IIP_{clone})} \qquad \text{Equation 12}$$

Supplementary Figures

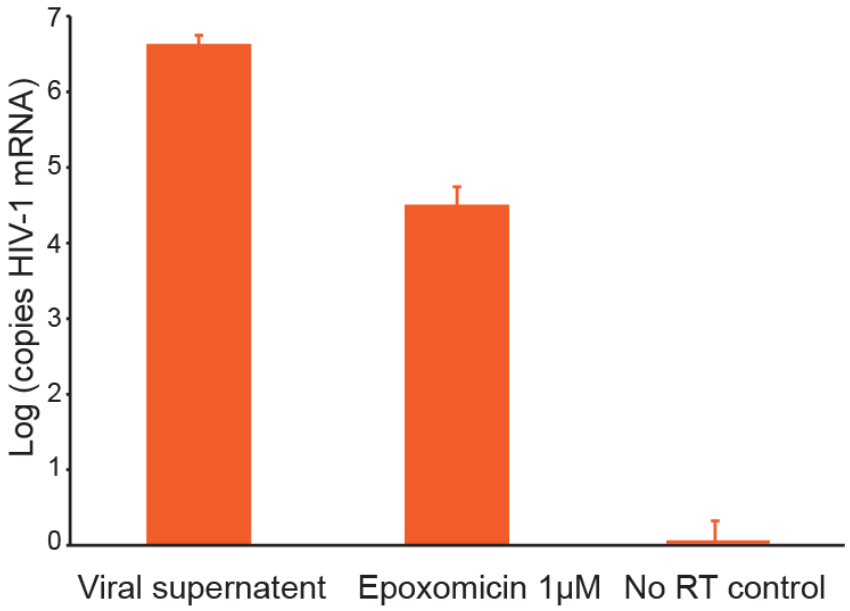

Supplementary Figure 1: An assay for virus production that is not affected by plasmid DNA. 293T cells were co-transfected with a plasmid carrying the NL4-3 provirus with GFP in the env ORF (NL4-3ΔEnv) and a vector expressing an X4-tropic envelope. At 48 hours post-transfection, viral RNA in the supernatant is measured by RT-qPCR. The 3' primer consisted of 25 dTs followed by 5 nucleotides (GAAGC) complementary to the last 5 nucleotides in the R region of the LTR. This primer hybridizes specifically to HIV-1 mRNAs (Shan et al., manuscript in preparation). The 5' primer anneals to a highly conserved region in the U3 region LTR. In control tubes in which reverse transcriptase was omitted, the signal detected was not significantly above the background. Epoxomicin is a proteasome inhibitor and has been shown to interfere with viral assembly and budding (30,31). Epoxomicin caused a 100-fold reduction in virus release. The assay sensitivity is 10 copies (Shan et al., manuscript in preparation).

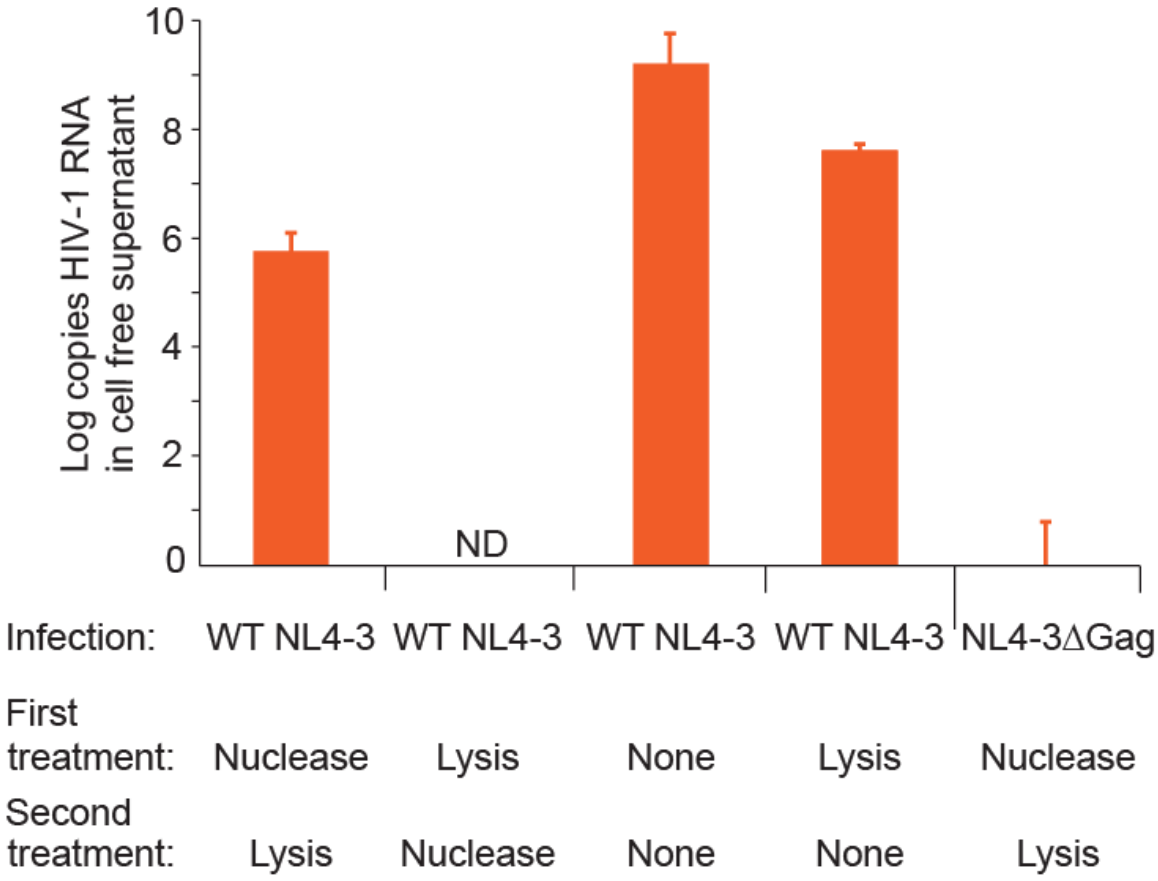

Supplementary Figure 2: Nuclease treatment prior to viral RNA extraction allows specific detection of intra-virion HIV-1 RNA. 293T cells were co-transfected with a plasmid carrying the NL4-3 provirus with GFP in the *env* ORF (NL4-3ΔEnv) and a vector expressing an X4-tropic envelope. At 48 hours post-transfection, the supernatant was treated with 1 unit/200μl of nuclease either before or after lysis of viral membranes with Triton X-100. After 10 minutes incubation in 37°, a second lysis buffer (AVL from Qigen) was added prior to RNA isolation. This second lysis buffer is highly denaturing which causes inactivation of the nuclease enzyme as well as lysis of the viral membrane in samples that were not previously lysed by the triton X-100. Viral RNA in the supernatant is measured by RT-qPCR using primer pairs described above. In control experiments, a viral construct with a stop codon in the reading frame of Gag (NL4-3ΔGag) was used. In the absence of Gag, virus particles do not assemble and bud from the producing cells,The signal detected in these samples is not significantly above the level of background. The assay sensitivity is 10 copies (Shan et al., manuscript in preparation). ND, none detected.

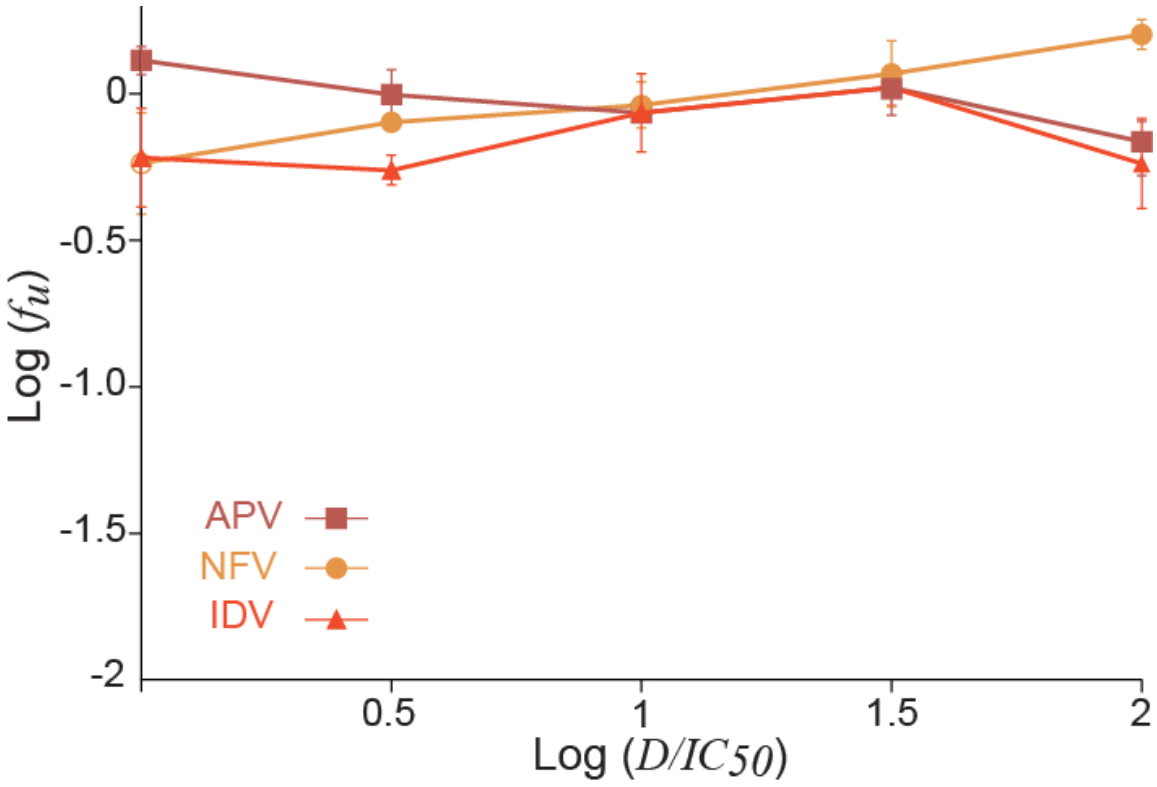

Supplementary Figure 3: PI treatment of virus-producing cells does not inhibit viral budding. 293T cells were co-transfected with NL4-3ΔEnv-GFP and a vector expressing an X4-tropic Env. Cells were then distributed in 96-well plates, and PIs were added. At 48 hours after transfection, supernatants were treated with 1 unit/150μl of nuclease to degrade free, extra-virion RNA. Viral RNA in the supernatant was measured by quantitative RT-PCR using primer-probe pair specific for HIV-1 mRNA. IC_{50} values refer to the overall PI IC_{50} measured in (2) and are 144.2 nM, 166.8 nM, and 90.9 nM for APV, NFV and IDV, respectively.

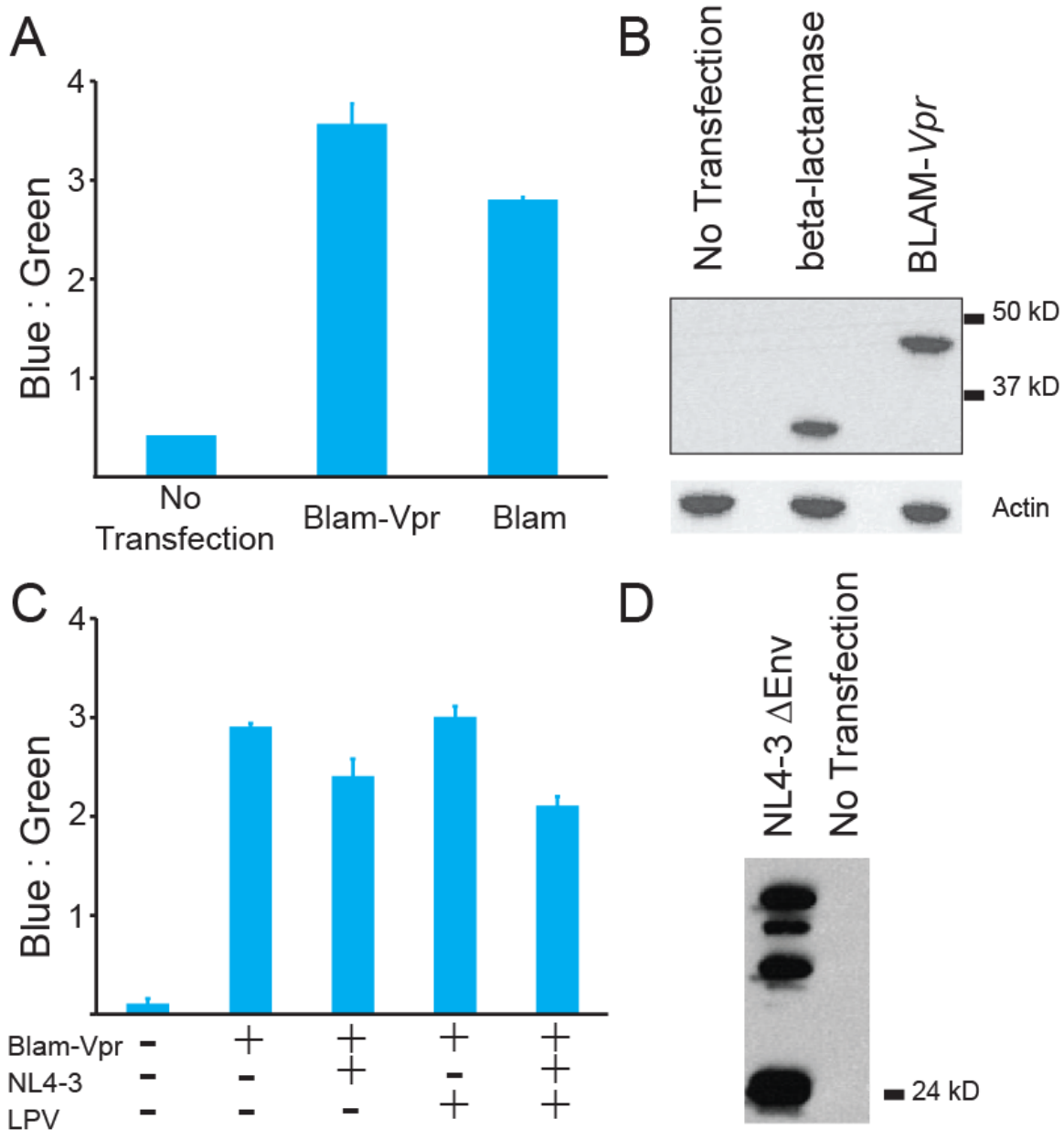

Supplementary Figure 4: The enzymatic activity of the BLAM-*Vpr* fusion protein is not dependant on cleavage by HIV-1 protease and is not affected by the action of PIs. **(A)** BLAM-*Vpr* fusion protein has the same level of enzymatic activity as the beta-lactamase enzyme. 293T cells were transfected with either Blam-*Vpr* or a beta-lactamase-encoding construct. At 24 hours post-transfection, the cells were incubated with the substrate CCF2-AM. The enzymatic activity was quantified as the ratio of blue to green color change by flow cytometry. **(B)** Western Blot analysis to assess expression of BLAM-*Vpr* and beta-lactamase in the cells used in A **(C)** The enzymatic activity of BLAM-*Vpr* is not dependent on the action of HIV-1 protease and is not affected by the action of PIs. 293T cells were transfected with Blam-*Vpr* alone or along with the NL4-3ΔEnvGFP

construct expressing HIV-1 protease in the presence or absence of 1 μM LPV. At 24 hours post-transfection, the cells were incubated with the substrate CCF2-AM. The enzymatic activity was quantified as the ratio of blue to green color change by flow cytometry. **(D)** Cells transfected with the NL4-3ΔEnvGFP construct express functional HIV-1 protease. 293T cells transfected with the NL4-3ΔEnvGFP were washed three times in cold PBS 24 hours after transfection. Cell lysates were analyzed via Western Blot for the presence of fully processed Capsid protein using an anti-p24 antibody.

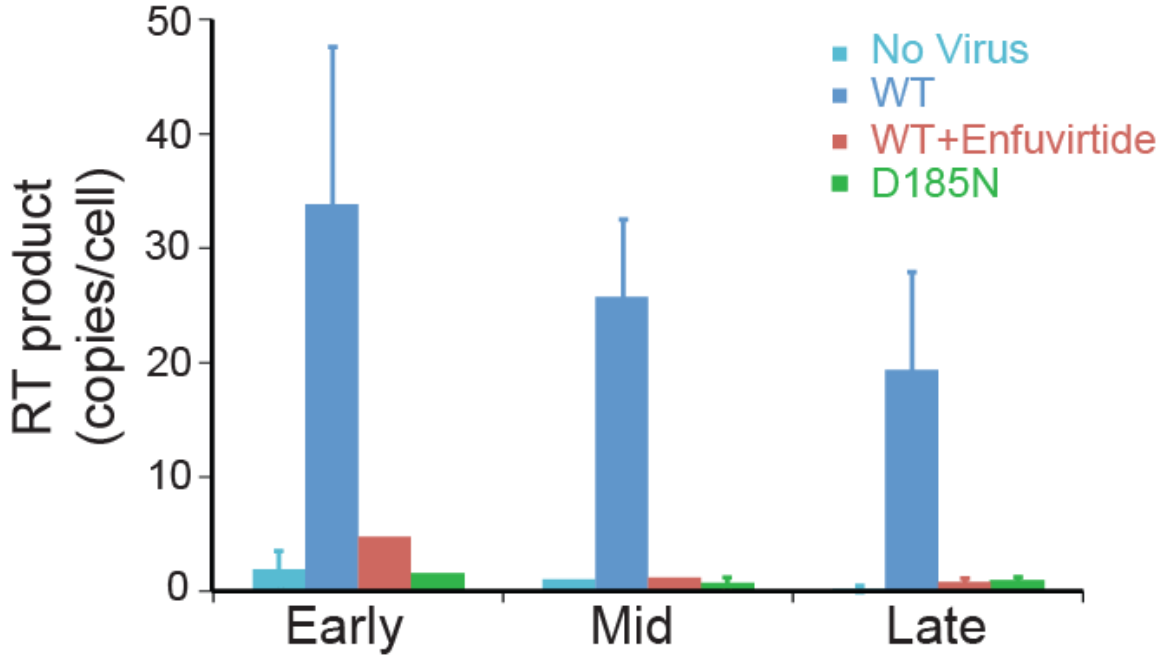

Supplementary Figure 5: Quantitation of HIV-1 early, middle, and late reverse-transcription products in primary $CD4^+$ T lymphoblasts 36 hours after infection. 293T cells were co-transfected with NL4-3ΔEnv and an X4-tropic envelope. Supernatants were collected at 48 hours and used to infect primary $CD4^+$ T lymphoblasts. At 36 hours after infection, $CD4^+$ T cells were washed and treated with nuclease to remove residual plasmid DNA. Cells were then washed 3x with cold PBS to remove the nuclease. Cells were then lysed, and DNA was isolated. Early, middle, and late RT products were quantified by qPCR (38). Treatment of cells with the fusion inhibitor enfuvirtide prior to the addition of virus prevented the appearance of RT products as did the use of virus with an inactivating D185N mutation in the active site of RT.

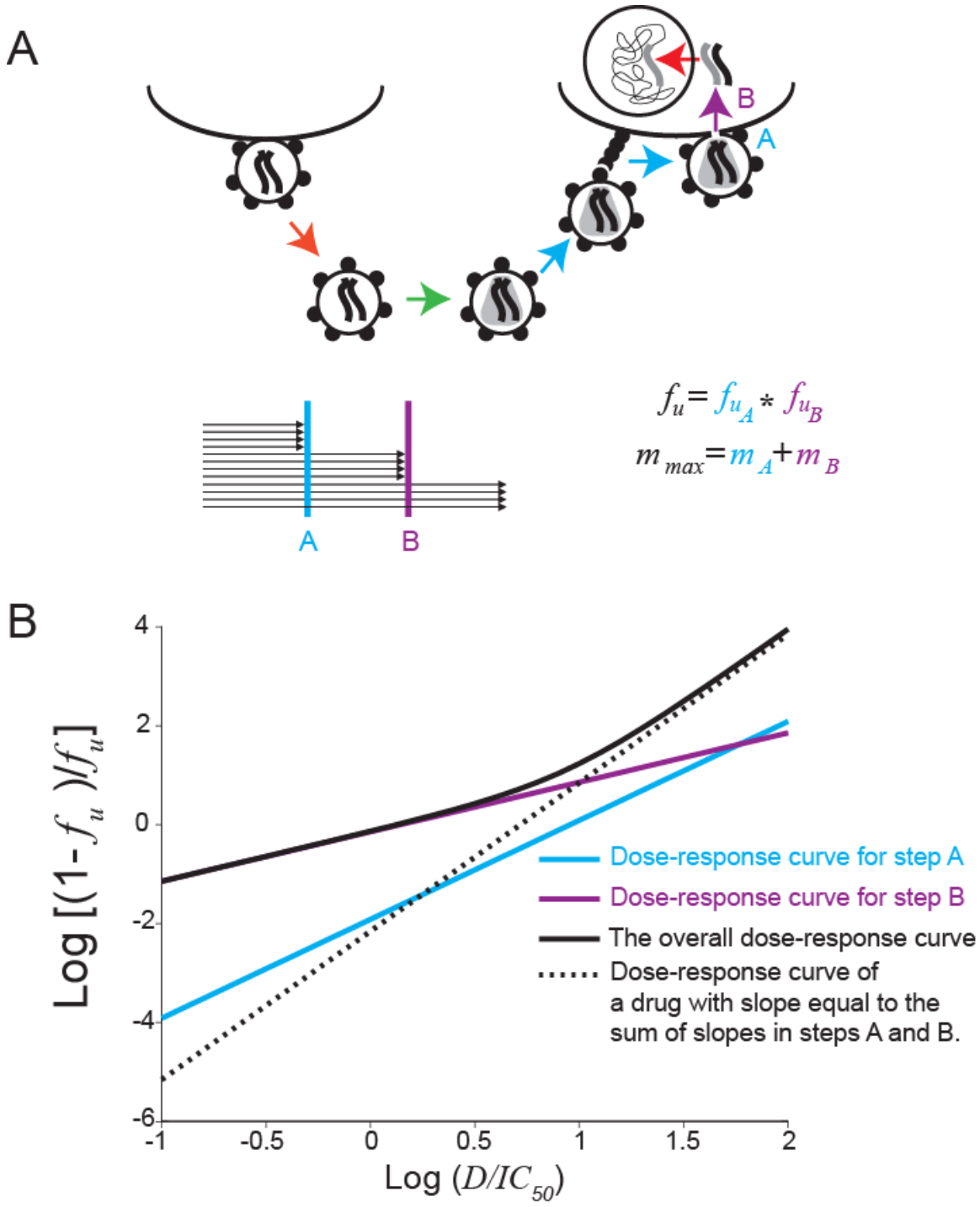

Supplementary Figure 6. The overall dose-response curve of a drug acting at two different steps of life cycle. **(A)** A hypothetical drug blocking two different steps of life cycle, A and B. Assuming that the inhibition at each step is independent of the previous step(s), Bliss model of drug-drug interaction (47) can be used to predict the overall fraction of viruses that can complete the life cycle (f_u) from the fraction of viruses that complete each individual step. **(B)** The overall median effect dose-response curve of a drug acting at two subsequent

steps of life cycle inflects concaves up to approximate the dose-response curve of a hypothetical drug with slope equal to the sum of the slopes at each individual step of the life cycle. The blue and purple curves are dose-response curves for the inhibition of steps A, and B, respectively. The solid black curve is the overall dose-response curve, and the dotted black curve is the dose-response curve of a hypothetical drug with slope equal to the slopes at steps A and B. (IC_{50A}, IC_{50B}, m_A and m_B used here are: 214 nM, 33 nM, 2, and 1, respectively).

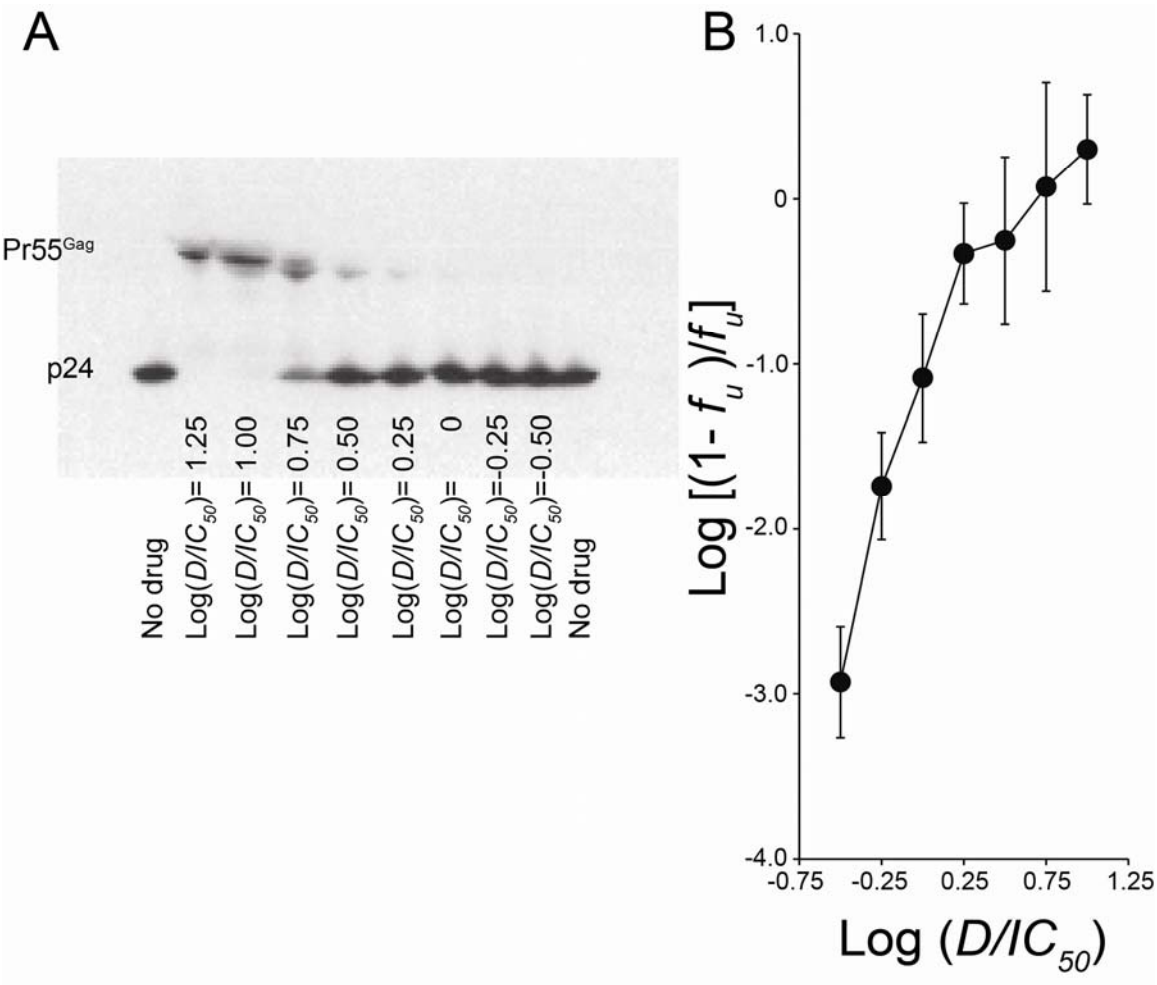

Supplementary Figure 7. Dose-response curve for PI-mediated inhibition of processing of Pr^{55Gag}. HEK 293T cells were co-transfected with an NL4-3ΔEnv vector expressing wild type *gag* and *pol* and with vectors expressing X4-tropic HIV-1 *env*. ATV was added to the cells at the indicated concentrations. Two days later, supernatants were analyzed using Western Blotting for p24 in triplicate. **(A)** A representative blot. **(B)** The intensities of the p24 bands were quantified using ImageJ software and the results plotted according to the median-effect model (Equation 2). Drug concentrations are normalized by previously measured IC50 value for inhibition of infectivity by ATV (13.6 nM, reference 2).

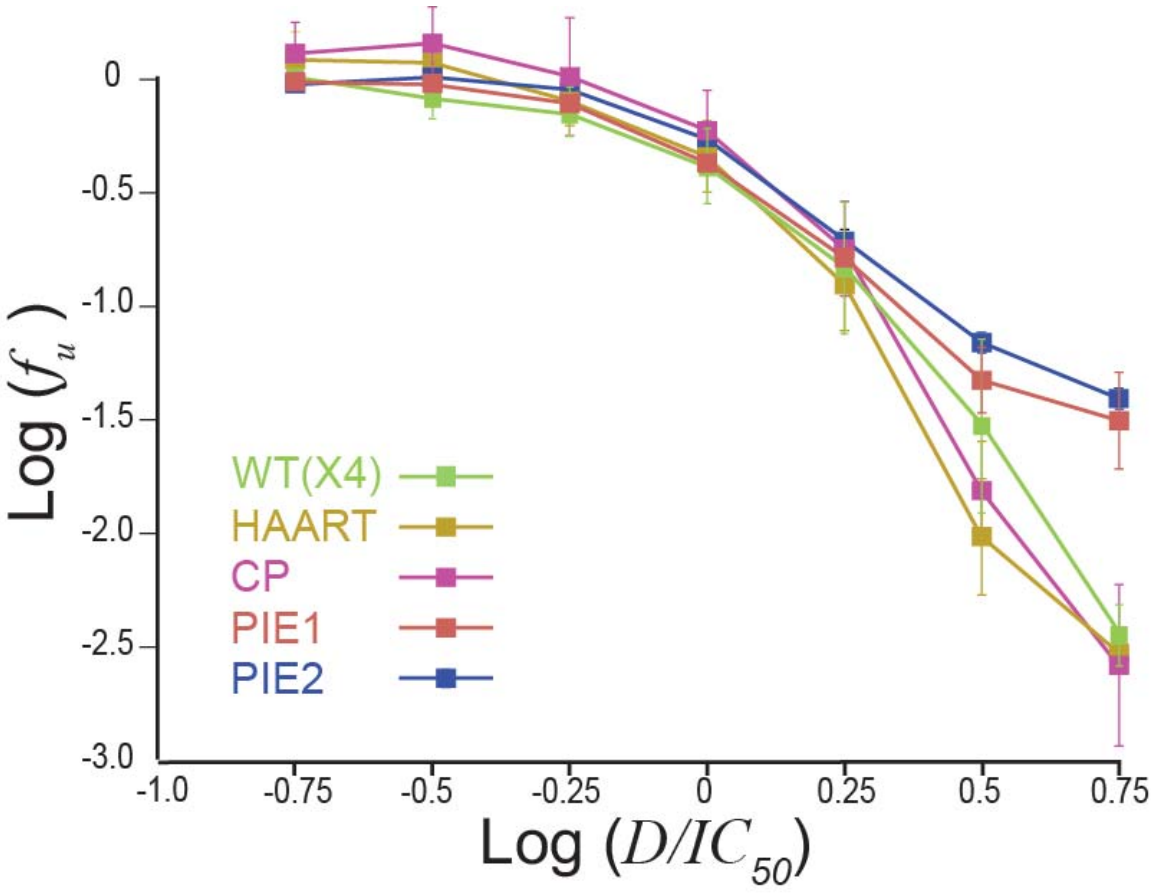

Supplementary Figure 8: Effect of mutations in the Envs cloned from patients who failed PI-containing regimens without evidence of major PI mutations in the protease gene on PI resistance. Full-length *env* was cloned from two patients with plasma HIV-1 RNA levels >50 copies/ml who were on PI-containing regimens and did not have evidence of PI-resistance mutations in the protease gene (PIE1 and PIE2) as well as from a patient who is taking HAART with a plasma HIV-1 RNA level <50 copies (HAART) and a treatment-naïve chronic progressor (CP). 293T cells were co-transfected with an NL4-3ΔEnv vector expressing wild type *gag* and *pol* and with vectors expressing either of the above Env constructs or a wild-type X4-tropic HIV-1 Env. Transfected cells were plated in 96-well plates, and PIs were added. Two days after transfection, supernatants were used to infect $CD4^+$ lymphoblasts. Three days later, the infection was quantified as the percentage of cells expressing GFP.

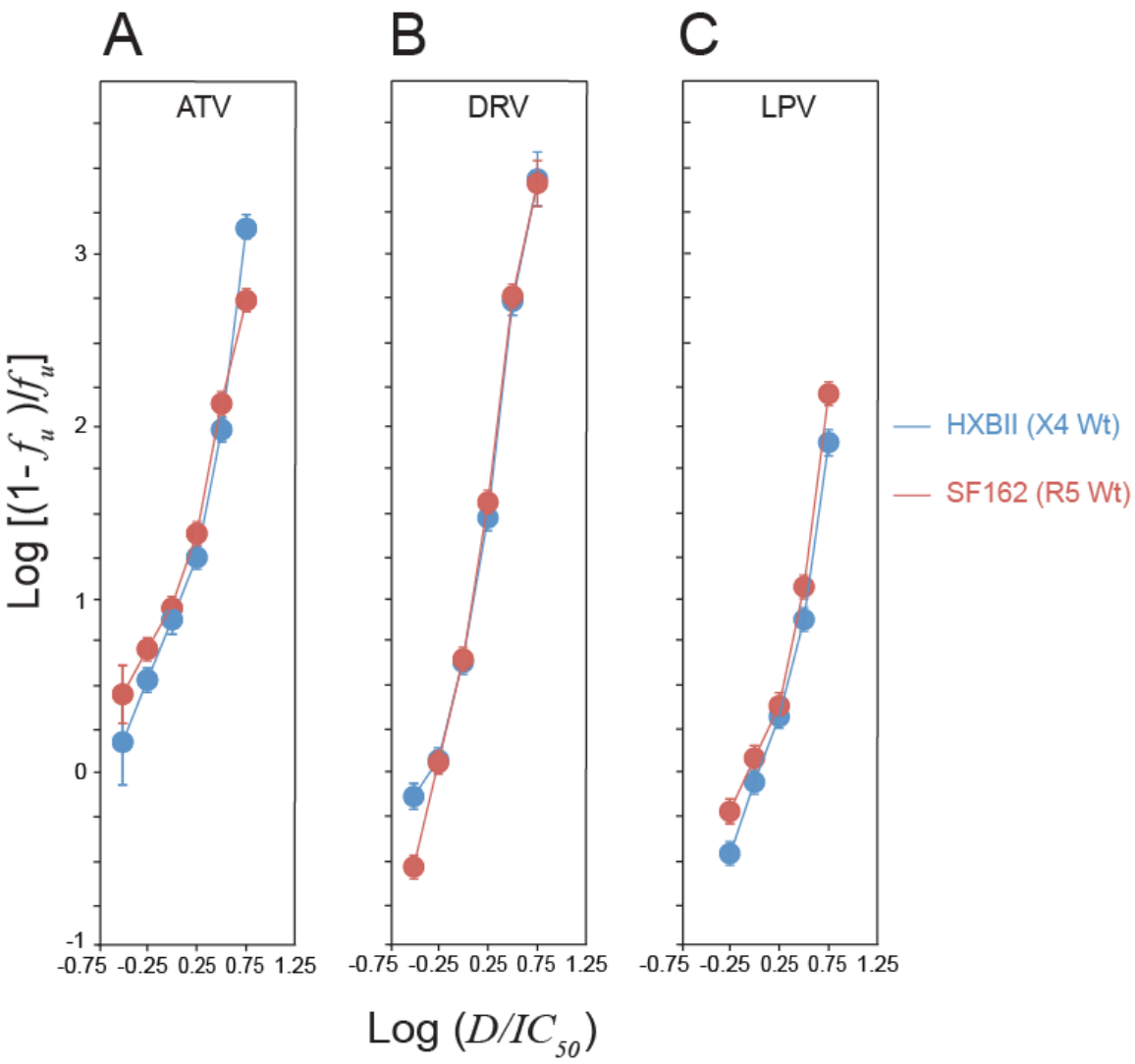

Supplementary Figure 9. The effect of Env tropism on PI dose-response curves. HEK 293T cells were co-transfected with an NL4-3ΔEnv vector expressing wild type *gag* and *pol* and with vectors expressing either R5- or X4-tropic HIV-1 Envs. Transfected cells were plated in 96-well plates, and the indicated PIs were added. Two days after transfection, supernatants were used to infect $CD4^+$ lymphoblasts. Three days later, the infection was quantified as the percentage of cells expressing GFP.

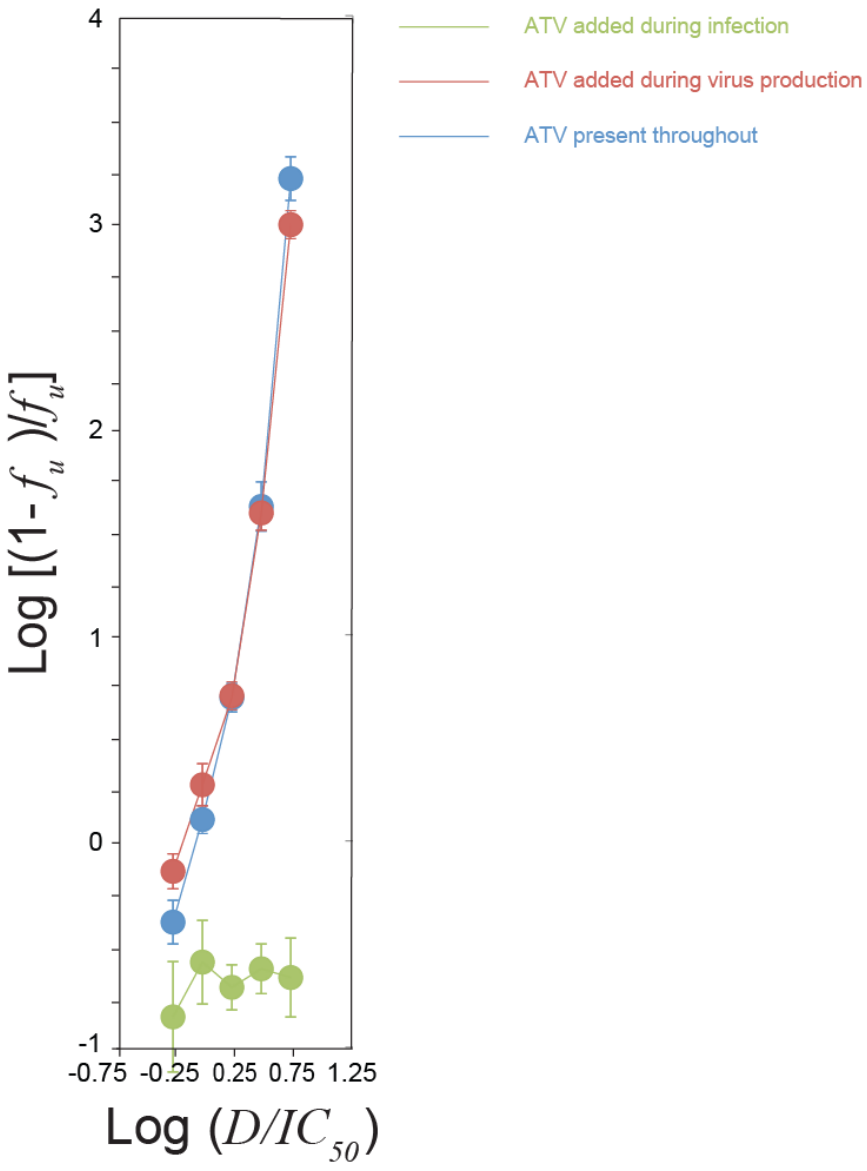

Supplementary Figure 10. Effect of adding PIs at different stages of viral life cycle. HEK 293T cells were co-transfected with an NL4-3ΔEnv vector expressing wild type *gag* and *pol* and with vectors expressing X4-tropic HIV-1 *env*. Two days later, supernatants were used to infect $CD4^+$ lymphoblasts. ATV was present at the indicated concentrations wither during virus production by HEK 293T cells, during the infection of $CD4^+$ T lymphoblasts, or both during virus production and infection of $CD4^+$ T lymphoblasts.

Supplementary Table 1. Patient characteristics.

Patient ID	Age	Sex	Race[a]	Plasma HIV-1 RNA (copies/ml)	CD4 count (cells/μl)	Current Regimen[b]	Known resistance mutations[c]	Previous antiretroviral treatment history[b]	Env clones	Source of clones
PIE1	33	M	AA	2031[d]	174[d]	TDF, FTC, DRV/r,	RT: K103N, M184V	AZT, 3TC, EFV, NFV, ATV/r	PIE1	plasma
PIE2	51	F	C	50,758[e]	199[e]	TDF, FTC, DRV/r, RAL	RT: D67N, K70R, V118I, M184V, K219Q, Pro: A71T Int: V151I	AZT,d4T, ddI, 3TC, NVP, IDV, LPV/r	CDS4, PIE2	plasma
PIE3	37	M	AA	35083[f]	130[f]	TDF, FTC, ATV/r	Pro: M36I	AZT, ABC, 3TC, LPV/r	TBL1	PBMC lysate
PIE4	32	F	AA	13036[g]	357[g]	TDF, FTC, ATV/r	RT: K103N	AZT, 3TC, LPV/r, EFV, TDF, FTC	15-9, 15-13, 15-17, 15-20, 15-22	plasma
PIE5	48	M	AA	434[g]	482[g]	TDF, FTC, DRV/r	Could not be amplified	LPV/r	16-2, 16-4	plasma
PIE6	44	M	AA	3796[h]	105[h]	DRV/r, ATV	RT: M41L, L74V, A98S, V108I, V118I, M184V, K103N, Y181C, T215Y Pro: A71T	AZT, ABC, TDF, ddI, d4T, 3TC, TDF, EFV, NVP, LPV/r	18-4, 18-5, 18-8, 18-9, 18-10, 18-14, 18-16	plasma
CP	40	F	AA	17,835[i]	360[i]	None	None	None	98rd12	
HAART	63	M	C	<50[j]	633[k]	EFV, ABC, 3TC	None	EFV, ABC, 3TC	2522	

[a]AA: African American; C: Caucasian

[b]Drug abbreviations: 3TC, lamivudine; ABC, abacavir; ATV/r, atazanavir boosted with ritonavir; AZT, zidovudine; d4T, stavudine; ddI, didanosine; DRV/r, darunavir boosted with ritonavir; EFV, efavirenz; FTC, emtricitabine; IDV, indinavir; LPV/r, lopinavir boosted with ritonavir; NFV, nelfinavir; RAL, raltegravir; TDF, tenofovir disoproxil fumarate,

[c]Resistance mutations detected on genotypic analysis. Mutations are classified as resistance mutations according to Reference 19 and the Stanford University HIV Drug Resistance Database (http://hivdb.stanford.edu/). For protease, the listed mutations are considered minor resistance mutations for ATV. RT, reverse transcriptase; Pro, protease; Int, integrase.

[d]Plasma HIV-1 RNA level and CD4 count determined 9 weeks prior to sampling for *env* cloning.

[e]Plasma HIV-1 RNA level and CD4 count determined 3 weeks prior to sampling for *env* cloning.

[f]Plasma HIV-1 RNA level and CD4 count determined 2 weeks prior to sampling for *env* cloning.

[g]Plasma HIV-1 RNA level and CD4 count determined same day as sampling for *env* cloning.

[h]Plasma HIV-1 RNA level and CD4 count determined 16 weeks prior to sampling for *env* cloning.

[i]Plasma HIV-1 RNA level and CD4 count determined 20 weeks prior to sampling for *env* cloning.

[j]Plasma HIV-1 RNA level determined 6 months prior to sampling for *env* cloning.

[k]CD4 count determined 6 months prior to sampling for *env* cloning.

Supplementary Table 2. Summary of the dose-response curve parameters for patient-derived Env clones.

Pt.	Clone	X4/ R5[a]	Drug	IC_{50} (nM)[b]	Slope[b]	IIP_{Cmax}[c]	Fractional Change in IIP_{Cmax}[d]	Replication Capacity[e]	Selective Advantage[f]
	HXB2	X4	ATV	9.09±0.61	2.68±0.38	6.26±0.26[h]	N/A	1.00	1.00
	SF162	R5	ATV	7.21±0.42	2.21±0.25	5.87±0.66	0.06±0.01	0.07±0.05	0.17±0.03
CP	98rd12	R5	ATV	NA[g]	NA[g]	NA[g]	NA[g]	0.48±0.06	NA[g]
HAART	2522	R5	ATV	NA[g]	NA[g]	NA[g]	NA[g]	0.29±0.03	NA[g]
	E1	X4	ATV	6.64±0.52	1.37±0.18	3.65±0.49	**0.42±0.06**	0.05±0.01	20.51±26.44
	E51	X4	ATV	6.39±1.05	1.04±0.29	2.78±0.77	**0.56±0.16**	0.06±0.00	170.15±317
PIE1	PIE1	R5	ATV	8.84±0.30	1.87±0.11	4.97±0.29	**0.21±0.01**	0.10±0.01	1.96±1.77
PIE2	PIE2	R5	ATV	3.40±0.51	0.49±0.09	1.32±0.25	**0.79±0.15**	0.01±0.00	987.18±830
PIE2	CDS4	R5	ATV	NA[g]	NA[g]	NA[g]	NA[g]	0.06±0.01	NA[g]
PIE3	TBL-1	R5	ATV	NA[g]	NA[g]	NA[g]	NA[g]	0.32±0.06	NA[g]
PIE4	15-9	R5	ATV	7.55±0.29	2.17±0.16	5.78±0.43	0.08±0.01	0.08±0.01	0.24±0.28
PIE4	15-13	R5	ATV	7.58±0.09	2.34±0.05	6.23±0.14	0.00±0.00	0.15±0.01	0.16±0.11
PIE4	15-17	R5	ATV	6.31±0.15	2.55±0.11	6.78±0.28	-0.08±0.00	0.16±0.01	0.05±0.04
PIE4	15-20	R5	ATV	6.06±0.16	2.26±0.10	6.02±0.27	0.04±0.00	0.17±0.01	0.28±0.25
PIE4	15-22	X4	ATV	6.67±0.09	2.37±0.06	6.31±0.15	-0.01±0.00	0.08±0.00	0.07±0.05
PIE5	16-2	X4	ATV	6.98±0.16	2.19±0.09	5.84±0.25	0.07±0.00	0.08±0.01	0.20±0.17
PIE5	16-4	R5	ATV	6.40±0.15	1.96±0.08	5.23±0.22	**0.16±0.01**	0.03±0.00	0.34±0.27
PIE6	18-4	R5	ATV	8.96±0.22	1.85±0.09	4.92±0.25	**0.21±0.01**	0.34±0.02	7.38±6.18
PIE6	18-5	R5	ATV	10.04±0.31	2.22±0.15	5.91±0.39	**0.06±0.00**	0.19±0.02	0.42±0.46
PIE6	18-8	R5	ATV	9.79±0.74	1.70±0.28	4.53±0.25	**0.28±0.05**	0.23±0.03	12.39±22.33
PIE6	18-9	R5	ATV	6.06±0.16	2.26±0.10	6.02±0.27	0.04±0.00	0.30±0.03	0.52±0.45
PIE6	18-10	R5	ATV	7.41±0.21	1.70±0.09	4.53±0.25	**0.28±0.02**	0.12±0.01	6.23±5.24
PIE6	18-14	R5	ATV	8.18±0.30	1.65±0.12	4.40±0.33	**0.30±0.03**	0.17±0.02	12.37±12.01
PIE6	18-16	R5	ATV	8.73±0.28	1.26±0.08	3.35±0.23	**0.46±0.04**	0.06±0.00	47.80±38.08
	HXB2	X4	LPV	37.87±1.44	2.28±0.19	5.91±0.19[h]	NA	1.00	1.00
	SF162	R5	LPV	30.85±1.65	2.26±0.27	5.96±0.71	-0.01±0.00	0.07±0.05	0.06±0.01
CP	98rd12	R5	LPV	NA[g]	NA[g]	NA[g]	NA[g]	0.48±0.06	NA[g]
HAART	2522	R5	LPV	NA[g]	NA[g]	NA[g]	NA[g]	0.29±0.03	NA[g]
	E1	X4	LPV	25.10±3.33	1.51±0.16	2.87±0.72	**0.51±0.13**	0.05±0.01	528.80±909.1
	E51	X4	LPV	24.90±1.76	1.06±0.14	2.82±0.38	**0.52±0.07**	0.06±0.00	352.60±343
PIE1	PIE1	R5	LPV	85.87±5.65	1.00±0.10	2.66±0.28	**0.55±0.06**	0.10±0.01	577.4±455
PIE2	PIE2	R5	LPV	25.10±3.33	1.08±0.17	2.87±0.28	**0.52±0.07**	0.01±0.00	73.95±72.15
PIE2	CDS4	R5	LPV	NA[g]	NA[g]	NA[g]	NA[g]	0.06±0.01	NA[g]
PIE3	TBL-1	R5	LPV	NA[g]	NA[g]	NA[g]	NA[g]	0.32±0.06	NA[g]
PIE4	15-9	R5	LPV	33.30±0.71	2.67±0.13	7.05±0.33	-0.19±0.01	0.08±0.01	0.01±0.01
PIE4	15-13	R5	LPV	25.85±1.18	2.45±0.24	6.45±0.63	-0.09±0.01	0.15±0.01	0.04±0.07
PIE4	15-17	R5	LPV	16.72±0.78	2.07±0.17	5.45±0.46	0.08±0.01	0.16±0.01	0.46±0.53
PIE4	15-20	R5	LPV	20.48±0.68	2.28±0.15	6.01±0.40	-0.02±0.00	0.17±0.01	0.13±0.13
PIE4	15-22	R5	LPV	16.69±0.59	2.00±0.13	5.28±0.33	0.11±0.01	0.08±0.00	0.32±0.28
PIE5	16-2	X4	LPV	26.49±0.68	2.43±0.13	6.41±0.36	-0.09±0.01	0.08±0.01	0.02±0.02
PIE5	16-4	X4	LPV	22.34±1.10	2.13±0.21	5.63±0.57	**0.05±0.00**	0.03±0.00	0.06±0.08
PIE6	18-4	R5	LPV	34.29±0.28	1.90±0.03	5.02±0.09	**0.15±0.01**	0.34±0.02	2.65±1.28
PIE6	18-5	R5	LPV	20.43±1.43	1.29±0.18	3.41±0.47	**0.42±0.06**	0.19±0.02	60.79±71.23
PIE6	18-8	R5	LPV	39.27±2.56	1.43±0.21	3.77±0.55	**0.36±0.05**	0.23±0.03	31.52±42.34
PIE6	18-9	R5	LPV	20.48±0.68	2.28±0.15	6.01±0.40	-0.02±0.00	0.30±0.03	0.24±0.24
PIE6	18-10	R5	LPV	32.11±1.88	1.58±0.16	4.17±0.43	**0.29±0.03**	0.12±0.01	6.36±6.96
PIE6	18-14	R5	LPV	33.99±1.01	1.62±0.09	4.27±0.23	**0.28±0.02**	0.17±0.02	7.42±5.07
PIE6	18-16	R5	LPV	45.42±2.32	1.13±0.13	2.97±0.33	**0.50±0.06**	0.06±0.00	51.27±45.27

[a]Coreceptor usage predicted by the Geno2Pheno HIV coreceptor usage prediction algorithm (68).

[b]Slope and IC_{50} were calculated by fitting a linear regression model to the plot of $log[(1- f_u)/f_u]$ vs. $log(D/IC_{50})$ (Equation 2). See Appendix 2 (Supplementary Material) for details. Higher slope values are obtained in analysis that considers the upward inflection in the median effect plots (see reference 4).

[c]IIP_{Cmax} is the number of logs of inhibition of single round of infection at C_{max} and was calculated using Equation 7 (Supplementary Material).

[d]Fractional change in IIP_{Cmax} (ΔIIP_{Cmax}) for a given Env clone is calculated using Equation 9 (Supplementary Material). A positive value indicates a drug-resistant clone, whereas a negative value indicates a clone that is more susceptible than wild type. The 95% confidence interval for ΔIIP_{Cmax} is calculated as [$\mu-1.96\times\sigma$, $\mu+1.96\times\sigma$], where μ is the mean and σ is the standard error of the mean for $\Delta IIP_{Cmax.}$ Clones with a 95% confidence interval for ΔIIP_{Cmax} that did not include zero for all three drugs tested are shaded.

[e]Replication capacity is the relative ability of a mutant virus to complete a single round of infection compared to the wild type in the absence of a drug. It is calculated according to Equation 11 (Supplementary Material).

[f]Selective advantage (SA) is calculated using Equation 12 (Supplementary Material).

[g]Clones were not analyzed for this drug.

[h]IIP_{Cmax} for the wild type HXB2 was calculated by combining the two dose-response curves for entry and post-entry steps, as described in Equations 3 and 4.